Malaysian Journal of Analytical Sciences, Vol 22 No 6 (2018): 1065 - 1077
DOI: https://doi.org/10.17576/mjas-2018-2206-17

MALAYSIAN JOURNAL OF ANALYTICAL SCIENCES
Published by The Malaysian Analytical Sciences Society
ISSN 1394 - 2506

OPTIMIZATION OF ACID DOPED POLYBENZIMIDAZOLE ELECTROLYTE MEMBRANE FOR HIGH-TEMPERATURE PEM FUEL CELL

(Pengoptimuman Asid Didopkan Membran Elektrolit Polibenzimidazol untuk Sel Bahan Api PEM Suhu Tinggi)

Md Ahsanul Haque[1, 2], Abu Bakar Sulong[1, 3]*, Edy Herianto Majlan[1], Kee Shyuan Loh[1], Teuku Husaini[1], Rosemilia Rosli[1]

[1]*Fuel Cell Institute,*
Universiti Kebangsaan Malaysia, 43600 UKM Bangi, Selangor, Malaysia
[2]*Department of Applied Chemistry and Chemical Engineering,*
Islamic University, Kushtia-7003, Bangladesh
[3]*Department of Mechanical and Materials Engineering,*
Universiti Kebangsaan Malaysia, 43600 UKM Bangi, Selangor, Malaysia

**Corresponding author: abubakar@ukm.edu.my*

Received: 27 July 2017; Accepted: 28 April 2018

Abstract

This study optimized the H_3PO_4 acid doping level (ADL) of polybenzimidazole (PBI) polymer electrolyte membranes using Taguchi method and characterized their ionic conductivity, contour plot and performed statistical regression analysis. Electrochemical impedance spectroscopic (EIS) analysis revealed that PBI copolymer-1 exposed better ionic conductivity among other membranes used. The maximum proton conductivity of PBI copolymer-1was recorded as 6.30 mS/cm at a doping temperature of 130 °C, doping time of 6 hours, and an operating temperature of 160 °C whereby, the optimum parameters were driven from the contour plot and signal to noise ratios effect of variable factors. The ionic conductivity showed differentiable dependency on the ADL and required high operating temperature for maximum conductivity. Therefore, the data recommends that the PBI copolymer-1 may be applicable as a proton exchange membrane for the high-temperature polymer electrolyte membranes fuel cell.

Keywords: acid doping level, polybenzimidazole, Taguchi method, contour plot, proton conductivity

Abstrak

Kajian ini mengoptimumkan tahap pendopan asid H_3PO_4 bagi membran polimer elektrolit polibenzimidazol (PBI) menggunakan kaedah Taguchi dan mencirikan kekonduksian elektronik, plot kontur dan melakukan analisis prestasi regresi statistik. Analisis spektroskopi elektrokimia impedans (EIS) membuktikan bahawa kopolimer-1 PBI mendedahkan ionik konduktiviti yang lebih baik berbanding membran lain yang digunakan. Proton konduktiviti maksimum kopolimer-1 PBI direkodkan pada 6.30 mS/cm pada suhu pendopan pada 130 °C, masa pendopan 6 jam, dan masa suhu operasi 160 °C, manakala parameter optimum didorong dari plot kontur dan isyarat kepada kesan nisbah hingar dari faktor variasi. Ionik konduktiviti menunjukkan perbezaan kebergantungan terhadap ADL dan memerlukan suhu operasi yang tinggi untuk konduktiviti yang maksimum. Oleh itu, data mencadangkan bahawa kopolimer-1 PBI berkemungkinan boleh diaplikasi sebagai membran penukaran proton untuk membran polimer elektrolit sel fuel bersuhu tinggi.

Kata kunci: tahap pendopan asid, polibenzimidazol, kaedah Taguchi, plot kontur, konduktiviti proton

Introduction

Today, green energy is considered to be the most desirable energy source for near future across countries. As such this energy approach not only challenges the use of CO_2 emission technique that has a major role for the global warming but also poses a concern on the limited reserve of the fossil fuel for future use. To address these issues, Sopian et al. [1] have suggested that the PEMFC is going to be the most popular and attractive alternative clean energy conversion devices in the near future applications for automotive, stationary, and portable sectors. In PEMFC, the proton exchange membrane remains separated from the anode and cathode, and thus required conduction of protons from one side to the other electrode side. Therefore, the expected proton conduction rate through the membrane is very important for the overall cell performance. Currently, many researchers are involving membrane development for a demonstration in PEMFC applications [2-4].

In a low operating temperature (usually < 80 °C) PEMFC, the perfluoro sulfonic acid (PFSA, Nafion) polymer membrane is commonly used as the electrolyte membrane due to its low ionic conductive resistance. Lufrano et al. [5] have mentioned some potential challenges of this technique. The challenges are, for example, it is expensive, and having a limited working temperature, dependent on humidity, and inadequate for longer cell operations. Additionally, during operation at high temperatures (usually 120–180 °C), the Nafion membrane acts like a nonconductive substance, because of the dryness in the conductive medium of the membrane at this high temperature ranges. To solve these complexities, Wieser et al. [6] and Zhang et al. [7] have introduced high thermo-chemical resistant alternative polymeric membranes such as polyimides, polysulfones, polybenzoxazoles, poly(ether, ether ketones), PBI (polybenzimidazole), AB-PBI, poly(2,5-benzimidazole), poly(2,2-m-(phenylene)-5,5 bibenzimidazole), pyridine-based PBI, and sulfo-based PBI, to preferable use in high temperature PEMFC applications. Figure 1 depicts the chemical structure of PBI membrane.

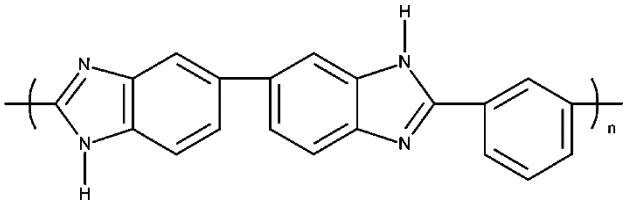

Figure 1. The chemical structure of polybenzimidazole.

PBI-based membranes have some potential advantages over Nafion in terms of price, thermal, mechanical, and chemical properties. However, the pristine PBI membrane has a low ionic conductivity due to lack of conduction media for proton transportation. It is only able to manage a high proton conduction system inside the membrane with the required amount of acid doping level (ADL). Jouanneau et al. [8] have shown that the PBI membranes are basic in nature because of having the N-H sites in the imidazole group. Therefore, this type of membrane could easily be modified by the treatment of strong acids such as H_3PO_4, H_2SO_4, HCl, HNO_3, $HClO_4$, and so on in order to enhance the proton conductivity [9]. However, the excess acid doping might be counter intuitive on the mechanical and thermal properties of the PBI membrane. Therefore, it would also be effective for the ADL of the PBI membrane to retain the prior criteria. In this study, we emphasized an optimum use of H_3PO_4 doping level of proton exchange membrane using Taguchi method. Additionally, we studied the relationship among variable factors using regression analysis and contour plot of PBI membrane.

Materials and Methods

We used pristine PBI copolymer-1 and PBI copolymer-2 electrolyte membrane (Fumatech BWT Group, Germany), the Nafion 212 membrane (DuPont, USA) and the chemical reagents, such as orthophosphoric acid, H_2O_2, and $FeSO_4$ (Sigma Aldrich, USA). All chemicals were used in laboratory analyzed grade.

Pristine PBI copolymer-1 and PBI copolymer-2 electrolyte membranes are ionic conductive and electronic nonconductive, despite their different molecular weight and thickness, although both are PBI based copolymer. In addition, Nafion 212 is commonly used PEM fuel cell application in the low working temperature range. In this

study, we compared PBI AM, PBI AP and Nafion 212 in terms of proton conductivity under high temperature. For proton conduction, it needs a less volatile solvent and high boiling point to support the conduction media, which increases the hoping of hydrogen bonds inside the membrane (Grothious mechanism) that is most likely to favor of proton transportation through the membrane [10]. PBI copolymer-1 and PBI copolymer-2 membranes were cut into small pieces that submerged in the orthophosphoric acid bath (85% concentration H_3PO_4) to get the expected proton conductivity. Prior to the acid doping, the PBI membrane was dried in a vacuum oven at 110 °C until a constant weight was reached, and the membrane thickness was recorded by the Mitutoyo-7321 (Japan) thickness gauge. Later on, the membrane was dipped into the acid bath for a certain period of time with a desirable temperature. The membrane thickness was increased due to gradually penetration of acid molecules. Next, the acid doped membrane was gently swept by a lab tissue to remove any unexpected residue or solvent, which was finally dried at 70 °C for 24 hours.

The proton conductivity of acid doped PBI copolymer-1, PBI copolymer-2, and Nafion 212 membranes was measured by the Autolab Potentiostat AUT84976 in context to the electrochemical impedance spectroscopic (EIS) analysis. The frequency ranges set were from 0.10 Hz to 1MHz, amplitude was 0.01, and the applied current ranged from 100 nA to 1 A. Using those parameters, we performed a Nyquist plot that helps find out the ionic resistance of that membrane. In this case, two Pt mesh probes were used to measure the proton conductivity through the membrane, according to the following equation (1) [11-12].

$$\alpha = L/RA \tag{1}$$

whereas σ is proton conductivity (S/cm), L is thickness of membrane (cm), R is = resistance of membrane (Ω) and A is membrane area πr^2 (cm^2); r is the radius of sample specimen.

The acid doping level (ADL) of the doped PBI membranes were determined on the basis of the ion exchange capacity (IEC). In addition, acid doped membranes were immersed in 2.0 M NaCl solution and kept overnight for H^+ ion exchange from the doped membrane. The resultant NaCl solution was titrated by a 0.02 M NaOH solution. The Phenolphthalein indicator was used to detect the endpoint. The membranes were protonated using 1.0 M HCl solution for several hours. After that, it was dried in an oven at 105°C until getting the constant weight. Therefore, the ADL of the doped membrane was calculated according to the following equation (2) [13-16].

$$\mathrm{ADL} = \frac{V_{NaOH} * S_{NaOH}}{W_{PBI}} \tag{2}$$

V_{NaoH} is volume of NaOH in ml, S_{NaoH} strength of NaOH in molarity, and W_{PBI} is dry weight of PBI membrane

Taguchi method is one of the well-known techniques, which can be used in a systematic optimization and efficient methodology process for a design of experiment (DoE) [17]. According to this method, L9 orthogonal array created the DoE as shown in Table 1. The acid doped PBI copolymer-1 membrane optimized the maximum ADL and the highest proton conductivity. In this case, three factors were considered doping time, doping temperature, and operating temperature at three levels. To get the optimum conditions, we made sure of the narrow and sharp analysis during the screening of all factors. Signal to noise ratios and orthogonal arrays are two major tools that were used to analyze the responses of DoE. In this study, "Larger is better" of S/N ratio was determined the steps according to the following equation (3) [18].

$$\frac{S}{N} = -10log\frac{1}{n}\sum y^2 \tag{3}$$

where, $\frac{S}{N}$ is signal to noise ratio, n is number of observations, and y is response.

Table 1. Taguchi design of experiment based on L9 orthogonal array

Exp. No	Doping Temperature	Doping Time	Operating Temperature
1	1	1	1
2	1	2	2
3	1	3	3
4	2	1	2
5	2	2	3
6	2	3	1
7	3	1	3
8	3	2	1
9	3	3	2

Responses comprised the statistical analysis of variances based on the regression analysis of the ADL and proton conductivity were performed in MINITAB 17 (software). The regression analysis refers to the correlation and interaction effect between the responses of ADL, as well as of proton conductivity.

Results and Discussion

Membrane selection

The proton conductivity is the most selective criterion of high temperature proton exchange membrane (PEM) fuel cell. The Nyquist plot that was introduced to measure the ionic conductivity of the membrane confirms the concurrency of the curve according to the $[R_S(C[R_{CT}Q])W]$ as an equivalent circuit that is shown in Figure 2(a and b). Figure 2(b) shows that the phase angle is close to zero at high frequency range. Therefore, the conductance C, and constant phase element Q are negligible impedance, since the impedance is inversely proportional to frequency [19, 20]. Whereas R_S represents the electrolyte resistance that was needed in the analysis of the membrane, R_{CT} refers the charge transfer resistance. However, the symbol of W indicates the infinite diffusion that was further confirmed by the Nyquist plot. During the conductivity measurement, the proton remained in diffusion throughout the membrane. The proton conductivity of each membrane was calculated by putting the value of electrolyte (polymer membrane) resistance (R_S), with their corresponding electrolyte membrane area (A), and thickness of electrolyte membrane (L) in equation (1). In case of the PBI copolymer-1, PBI copolymer-1, and Nafion 212 electrolyte membranes, the recorded proton conductivities were 5.83, 4.85, and 3.34 mS/cm respectively, at 120 °C temperature. Table 2 shows the values of proton conductivity and equivalent circuit elements. Among of them, the PBI copolymer-1 membrane exhibits the maximum proton conductivity. Since the PBI copolymer-1 membrane absorbed the high ADL content compared to the PBI copolymer-2 membrane which can accelerate the conduction medium at a high temperature. In addition, greater thickness and different molecular weight can explain for high acid absorbing affinity [21]. In contrast, the Nafion 212 membrane exhibits relatively lower conductivity compared to the both PBI membranes at high temperature. Since the Nafion 212 was dehydrated at 120 °C temperature (over the water boiling point), this was insufficient to support the conduction media for proton conduction. Taken together, it may be concluded that the PBI copolymer-1 membrane is the most promising candidate for high temperature PEM fuel cell.

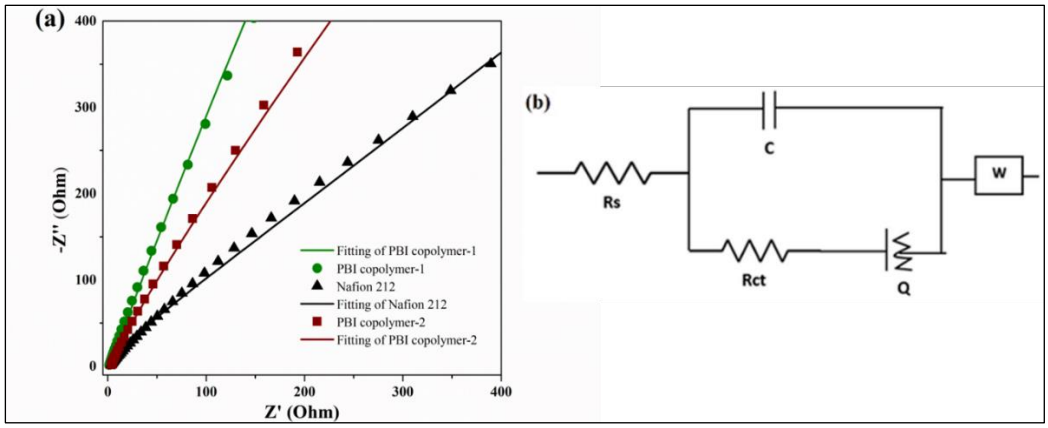

Figure 2. (a) Nyquist plot with fitting curve of membranes and (b) equivalent circuit

Table 2. Proton conductivity and equivalent circuit report

Items	Thickness L (cm)	Area A (cm^2)	Resistance R_s (Ohm)	Conductance (C)	Constant Phase Element (Q)	Chi-Square (x^2)	Conductivity (mS/cm)	Estimate Error (%)
Nafion 212	0.0036	0.64	1.687	1.2E-06	4.4E-05	< 0.01	3.34	1.33
PBI copolymer-1	0.0052	0.64	1.394	1.6E-06	2.0E-05	< 0.01	5.83	1.78
PBI copolymer-2	0.0051	0.64	1.642	2.2E-06	5.0E-05	< 0.01	4.85	1.56

Factor screening

The Nyquist plot depicts that the proton conductivity increases due to the lowering of membrane resistance at high doping temperature as shown in Figure 3(a). Figure 3(b) clearly shows that the conductivity and ADL gradually increase as a function of doping temperature, and the maximum outcomes occur doping temperature of 120 °C. Because of the acid absorbing power of membranes are increased under high doping temperature. Furthermore, the factor screening for narrow and sharp analysis was performed such a way so that one variable was varied while other two variables were kept constant. For example, the doping temperature was increased by 20 °C started from 80 °C to 120 °C while the doping time of 6 h and operating temperature of 120 °C were kept constant. In these preparations, the maximum conductivity and ADL were recorded at 4.36 mS/cm and 10.6 (mol/repeating unit), respectively.

Figure 4(a) shows that the doping time of 6 h screen out in terms of proton conductivity and ADL responses. Figure 4(b) shows that ADL and conductivity increase abruptly at the beginning stages. ADL content does not appreciably increase as a function of doping time increment, because of the membrane has saturated by acid doping. Similarly, the conductivity does not show significant improvement to further progress of doping time.

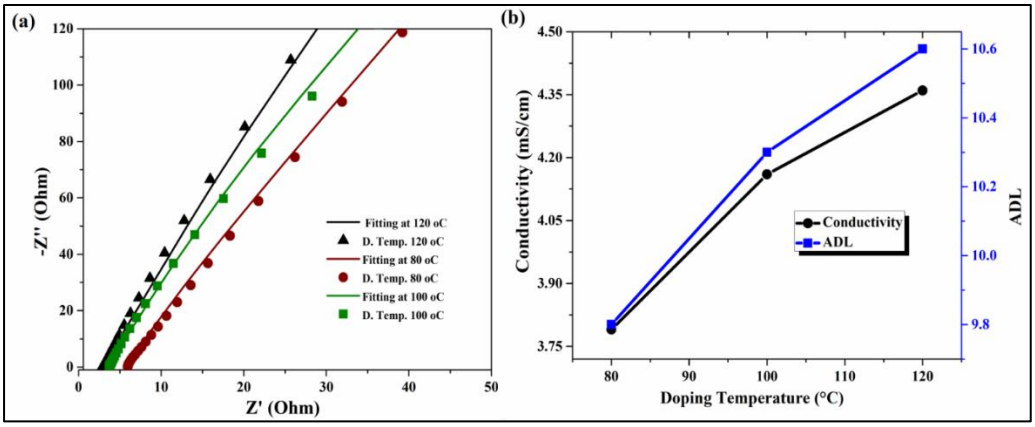

Figure 3. (a) Nyquist plot with fitting curve of PBI copolymer-1 at different doping temperatures and (b) corresponding proton conductivity and ADL

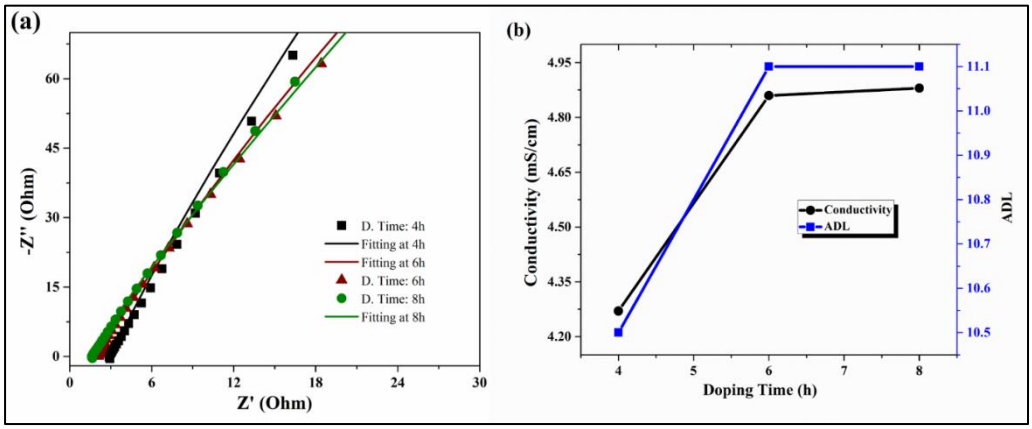

Figure 4. (a) Nyquist plot with fitting curve of PBI copolymer-1 at different doping time and (b) corresponding proton conductivity and ADL

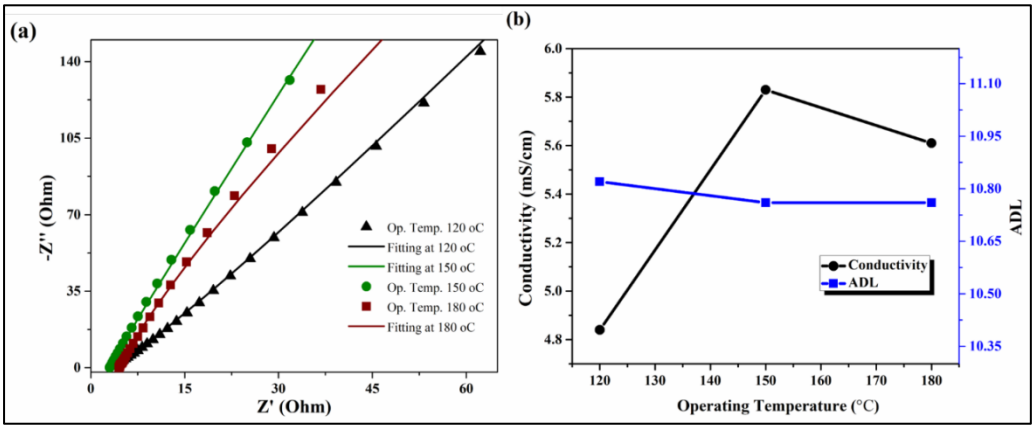

Figure 5. (a) Nyquist plot with fitting curve of PBI copolymer-1 at different operating temperatures and (b) corresponding proton conductivity and ADL

Operating temperature is the most significant factor in terms of proton conductivity due to its huge impact on the impedance, i.e. the conductivity of the membrane as shown in Figure 5(a). At the beginning stage, the conductivity increases as a function of operating temperature. Figure 5(b) reflects that the maximum conductivity recorded at 5.83 mS/cm under 150 °C operating temperature can be considered as a screening level for further analysis. The conductivity again decreases at high operating temperature. This is because it may fairly be changing tendency from phosphoric acid (H_3PO_4) to pyrophosphoric acid ($H_4P_2O_7$) which is less conductive than phosphoric acid [22]. In contrast, ADL content shows the steady state during different operating temperatures that were used. It is possible because the operating temperature of ADL refers the heat treatment of acid doped membrane and hence observes the effect of ADL content (like acid leaching, dryness etc.) of the membrane.

Taguchi optimization

Based on DoE, the outcomes of ADL, conductivity and their analyzed data were tabulated in Table 3, along three variable factors such as doping temperature, doping time, and operating temperature. Figure 6 demonstrations the Nyquist plot to measure the conductivity for all respective observations. Among of them, Obs-5 represents the maximum conductivity as 6.31 (mS/cm) under doping temperature 120 ℃, doping time 6 hours and operating temperature 160 ℃. Moreover, outcomes of ADL and conductivity were transformed into the signal to noise (S/N) ratios using equation (3) to select the optimum parameters. In this case, it has been considered that the "larger is the best". The main effects have been plotted for the ADL and conductivity of the S/N ratios that is shown in Figure 7(a) and 7(b).

Table 3. Optimization of ADL and conductivity based on DoE

Exp. No	Doping Temp. (°C)	Doping Time (h)	O. Temp. (°C)	ADL	S/N-1 Ratio of ADL	Conductivity (mS/cm)	S/N-2 Ratio of Conductivity
Obs-1	110	5	140	10.3	20.2567	5.07	14.1002
Obs-2	110	6	150	10.7	20.5061	5.72	15.1479
Obs-3	110	7	160	10.6	20.5877	5.80	15.2686
Obs-4	120	5	150	10.7	20.6685	5.56	14.9015
Obs-5	120	6	160	11.1	20.9065	6.31	16.0006
Obs-6	120	7	140	11.2	20.9065	5.69	15.1022
Obs-7	130	5	160	10.7	20.6685	5.93	15.4611
Obs-8	130	6	140	11.2	21.0616	5.74	15.1782
Obs-9	130	7	150	11.2	20.9844	6.11	15.7208

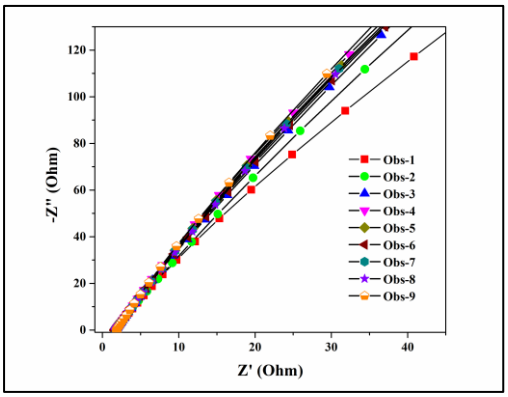

Figure 6. Nyquist plot of membrane for different observation of DoE

Figure 7(a) and Table 4 exhibit that the doping temperature and doping time great influencing factors on the ADL outcome. For ADL, the optimum factors were considered the doping temperature of 130 °C (level 3) and doping time of 6 hours (level 2). These values were obtained from the main effect plot of S/N ratios. In fact, the operating temperature is no appreciable effect on ADL outcome, and therefore it has no more significant effect on the S/N ratios. Similarly, Figure 7(b) and Table 5 reveal that the effect of factors on the conductivity responses to select optimum conditions. In this case, optimum conditions were obtained, such as doping temperature at 130 °C (level 3), doping time at 6 hours (level 2), and operating temperature at 160 °C (level 3).

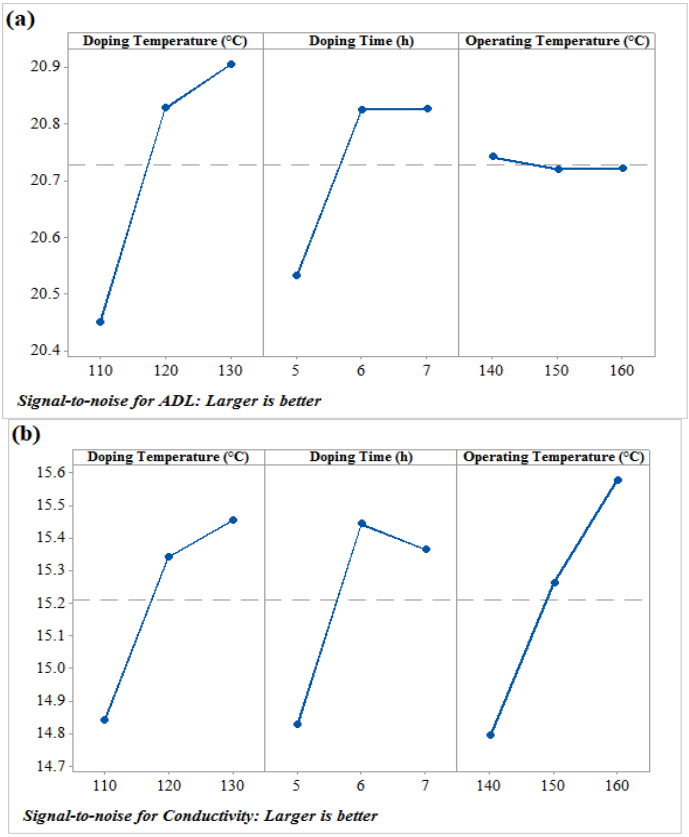

Figure 7. The main effect plot for S/N ratios of (a) ADL and (b) proton conductivity

Table 4. Signal-to-Noise (S/N) responses table for ADL

Level	Doping Temp. (°C)	Doping Time (h)	O. Temp. (°C)
1	20.45	20.53	20.74
2	20.83	20.82	20.72
3	20.90	20.83	20.72
Delta	0.45	0.29	0.02
Rank	1	2	3

Table 5. Signal-to-Noise (S/N) responses table for conductivity

Level	Doping Temp. (°C)	Doping Time (h)	O. Temp. (°C)
1	14.84	14.82	14.79
2	15.33	15.44	15.26
3	15.45	1536	15.58
Delta	0.61	0.62	0.78
Rank	3	2	1

Regression analysis

The regression equation has expressed the relationship among the variable parameters in a bid to evaluate the ADL and conductivity for any combination of factors at a level in a particular range. Based on the regression model, the error factors of ADL and conductivity were measured 1.33% and 1.34% using the optimum factors level through regression equations (4) and (5), respectively [23]. These results express the responses of ADL and conductivity that were measured in a systematic and scientific way. The multiple linear regression equations (4) and (5) were formulated for the ADL and conductivity using the MINITAB 17 software as following as [24, 25].

$$ADL = 6.63 + 0.02833\ D_{Temp} + 0.1833\ D_{Time} - 0.00167\ O_{Temp} \quad (4)$$

$$Conductivity = -1.49 + 0.01983\ D_{Temp} + 0.1717\ D_{Time} + 0.02567\ O_{Temp} \quad (5)$$

ADL regression results were tabulated in Table 6. It shows the different P values of different factors such as doping temperature, doping time, and operating temperature are 0.026 (<0.05), 0.010 (<0.05), and 0.823 (>0.05), respectively. It is very important in terms of lower (<0.05) P values that have a significant effect on the outcome. However, large P values (>0.05) have no significant effect on the results. Based on the P value, it is clear that the doping temperature and doping time have a huge effect on ADL outcome. Furthermore, it was studied the contour plot of ADL *vs.* respective factors that shown in Figure 8 (a-c), whereas; green colour represents the more reactive factorial effect on ADL and the blue colour represents the less reactive factors. Based on the contour plot, it may easily be concluded that the doping temperature and doping time are the influencing factors on ADL.

Table 6. Analysis of variance for ADL

Source	DF	Adj SS	Adj MS	F-Value	P-Value
Regression	3	0.685000	0.228333	7.58	0.026
Doping Temp. (°C)	1	0.481667	0.481667	16.00	0.010
Doping Time (h)	1	0.201667	0.201667	6.70	0.049
O. Temp. (°C)	1	0.001667	0.001667	0.06	0.823
Error	5	0.150556	0.030111		
Total	8	0.835556			

Similarly, it may also explain the effect P of values on the conductivity responses. Table 7 shows the P values for the doping temperature, doping time, and operating temperature such as 0.044, 0.069, and 0.018, respectively. In this case, all factors have a significant effect on the conductivity due to their low P values which are less than 0.50. In addition, the contour plot of conductivity depicts in Figure 8 (d-f), whereas; doping temperature and doping time had an approximately analogous effect on conductivity. However, the operating temperature was a higher impact on conductivity. Therefore, conductivity is dependent on factors according to priorities such as operating temperature>doping time>doping temperature.

Table 7. Analysis of variance for conductivity

Source	DF	Adj SS	Adj MS	F-Value	P-Value
Regression	3	0.8081	0.26937	8.14	0.023
Doping Temp. (°C)	1	0.2360	0.23602	7.14	0.044
Doping Time (h)	1	0.17682	0.17682	5.35	0.069
O. Temp. (°C)	1	0.3953	0.39527	11.95	0.018
Error	5	0.1654	0.03308		
Total	8	0.9735			

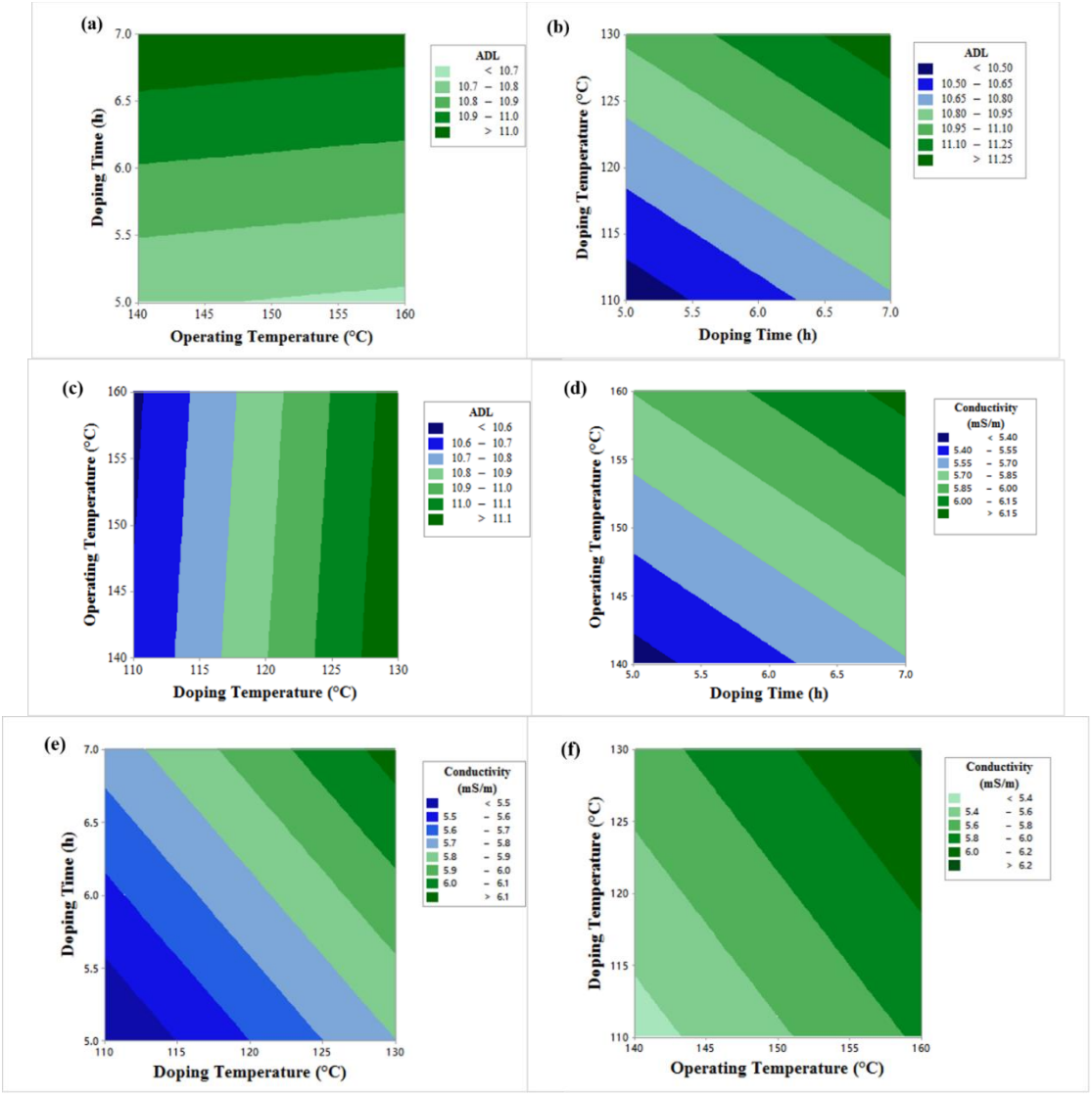

Figure 8. The contour plot of ADL at considering factors between (a) operating temperature *vs* doping time, (b) doping time *vs* doping temperature and (c) doping temperature *vs* operating temperature. The contour plot of proton conductivity for (d) operating temperature *vs* doping time, (e) doping temperature *vs* doping time and (f) doping temperature *vs* operating temperature

Confirmation test

The confirmation test is used to verify the experimental results with the predicted value. If the optimal combination of parameters and their levels coincidently match with one of the experiments of the DoE, then a confirmatory test is not required. In this study, the confirmation test is required due to the optimum combination of factors and their levels are not available to any individual observation in the DoE. The predicted value of the ADL and conductivity at optimum conditions were measured by adding the average performance to the contribution of each parameter at the optimum level for ADL and conductivity using the following equations (6) & (7), respectively [26-28].

$$Y_{ADL} = T_{avg} + (D.\ Time_{opt} - T_{avg}) + (D.\ Temp_{opt} - T_{avg}) \quad (6)$$

$$Y_{con} = T_{avg} + (D.\ Time_{opt} - T_{avg}) + (D.\ Temp_{opt} - T_{avg}) + (O.\ Temp_{opt} - T_{avg}) \quad (7)$$

whereas, Y_{ADL} is the predicted value of ADL, Y_{con} is the predicted value of conductivity, T_{avg} is the grand total average performance, D. $Time_{opt}$ is the doping time factor average at optimum level, D. $Temp_{opt}$ is the doping temperature factor average at optimum level, and O. $Temp_{opt}$ is the operating temperature factor average at optimum level. During the calculation of the predicted value of ADL and conductivity, it was substituted the respective values in above equations. The experimental and predicted results are shown in Table 8 and Table 9 for the confirmation of ADL and conductivity, respectively.

Table 8. Confirmation test for ADL

Opt. Level	Exp. Level	Predicted	Experimental Value			
			Obs-1	Obs-2	Obs-3	Average
A3, B2 (excluded C3)	A3, B2 (excluded C3)	11.2	11.1	11.4	11.3	11.3

Table 9. Confirmation test for conductivity

Opt. Level	Exp. Level	Predicted	Experimental Value			
			Obs-1	Obs-2	Obs-3	Average
A3, B2, C3	A3, B2, C3	6.19	6.36	6.25	6.29	6.30

Conclusion

This study suggested that PBI copolymer-1 is the most promising candidate for high-temperature PEM fuel cell application compared with PBI copolymer-2 and Nafion 212 due to convenient proton conductivity and acid absorbing capacity. The variable factors such as doping temperature, doping time, and operating temperature including three levels were considered for the Taguchi optimization of ADL and conductivity responses. The maximum ADL and ionic conductivity have measured 11.3 and 6.30 mS/cm under optimized conditions respectively. In addition, proton conductivity increases with increasing ADL. However, ADL depends on acid doping time and doping temperature. The contour plot is suggested that the variable factors of conductivity can be arranged high to low priorities as operating temperature>doping time>doping temperature.

Acknowledgement

This work has been financially supported by the Universiti Kebangsaan Malaysia under the Grant AP-2013-010 and TRGS/2/3014/UKM/02/4/1. The authors would like to thanks the university administration for the financial support.

References

1. Sopian, K. and Daud, W. R. W. (2006). Challenges and future developments in proton exchange membrane fuel cells. *Renewable Energy*, 31(5): 719-727.
2. Haque, M. A., Sulong, A. B., Rosli, R. E., Majlan, E. H., Shyuan, L. K. and Mashud, M. A. A. (2015). Measurement of hydrogen ion conductivity through proton exchange membrane. *IEEE International WIE* Conference: pp. 552-555.

3. Tang, Z., Ng, H. Y., Lin, J., Wee, A. T. and Chua, D. H. (2010). Pt/CNT-based electrodes with high electrochemical activity and stability for proton exchange membrane fuel cells. *Journal of The Electrochemical Society*, 157(2): 245-250.
4. Shao, Y., Yin, G., Gao, Y. and Shi, P. (2006). Durability study of Pt/C and Pt/CNTs catalysts under simulated PEM fuel cell conditions. *Journal of the Electrochemical Society*, 153(6): 1093-1097.
5. Lufrano, F., Baglio, V., Staiti, P., Arico, A. S. and Antonucci, V. (2006). Development and characterization of sulfonated polysulfone membranes for direct methanol fuel cells. *Desalination*, 199(1-3): 283-285.
6. Wieser, C. (2004). Novel polymer electrolyte membranes for automotive applications–requirements and benefits. *Fuel Cells*, 4(4): 245-250.
7. Zhang, H. and Shen, P. K. (2012). Recent development of polymer electrolyte membranes for fuel cells. *Chemical Reviews*, 112(5): 2780-2832.
8. Jouanneau, J., Mercier, R., Gonon, L. and Gebel, G. (2007). Synthesis of sulfonated polybenzimidazoles from functionalized monomers: Preparation of ionic conducting membranes. *Macromolecules*, 40(4): 983-990.
9. Xing, B., and Savadogo, O. (1999). The effect of acid doping on the conductivity of polybenzimidazole (PBI). *Journal of New Materials for Electrochemical Systems*, 2: 95-102.
10. Haque, M. A., Sulong, A. B., Loh, K. S., Majlan, E. H., Husaini, T. and Rosli, R. E. (2017). Acid doped polybenzimidazoles based membrane electrode assembly for high temperature proton exchange membrane fuel cell: A review. *International Journal of Hydrogen Energy*, 42(14): 9156-9179.
11. Chang, H. Y., and Lin, C. W. (2003). Proton conducting membranes based on PEG/SiO_2 nanocomposites for direct methanol fuel cells. *Journal of Membrane Science*, 218(1): 295-306.
12. Chang, H. Y., Thangamuthu, R. and Lin, C. W. (2004). Structure–property relationships in PEG/SiO_2 based proton conducting hybrid membranes—A^{29} Si CP/MAS solid-state NMR study. *Journal of membrane science*, 228(2): 217-226.
13. Navessin, T., Eikerling, M., Wang, Q., Song, D., Liu, Z., Horsfall, J., and Holdcroft, S. (2005). Influence of membrane ion exchange capacity on the catalyst layer performance in an operating PEM fuel cell. *Journal of the Electrochemical Society*, 152 (4): 796-805.
14. Thiam, H. S., Daud, W. R. W., Kamarudin, S. K., Mohamad, A. B., Kadhum, A. A. H., Loh, K. S. and Majlan, E. H. (2013). Nafion/Pd–SiO_2 nanofiber composite membranes for direct methanol fuel cell applications. *International Journal of Hydrogen Energy*, 38(22): 9474-9483.
15. Wang, J., Zhang, H., Jiang, Z., Yang, X. and Xiao, L. (2009). Tuning the performance of direct methanol fuel cell membranes by embedding multifunctional inorganic submicrospheres into polymer matrix. *Journal of Power Sources*, 188(1): 64-74.
16. Kang, S., Zhang, C., Xiao, G., Yan, D., and Sun, G. (2009). Synthesis and properties of soluble sulfonated polybenzimidazoles from 3,3′-disulfonate-4,4′-dicarboxylbiphenyl as proton exchange membranes. *Journal of Membrane Science*, 334(1): 91-100.
17. Phadke, M. S. (1995). Quality engineering using robust design. Prentice Hall PTR.
18. Vankanti, V. K. and Ganta, V. (2014). Optimization of process parameters in drilling of GFRP composite using Taguchi method. *Journal of Materials Research and Technology*, 3(1): 35-41.
19. Leong, J. X., Daud, W. R. W., Ghasemi, M., Ahmad, A., Ismail, M., and Liew, K. B. (2015). Composite membrane containing graphene oxide in sulfonated polyether ether ketone in microbial fuel cell applications. *International Journal of Hydrogen Energy*, 40(35): 11604-11614.
20. Song, X., Ren, S., Yang, Y., Guo, Y., Jing, H., Mao, Q., and Hao, C. (2017). Polyaniline-based electrocatalysts through emulsion polymerization: Electrochemical and electrocatalytic performances. *Journal of Energy Chemistry*, 26(1): 182-192.
21. Yang, J. S., Cleemann, L. N., Steenberg, T., Terkelsen, C., Li, Q. F., Jensen, J. O., Hjuler, H. A., Bjerrum, N. A. and He, R. H. (2014). High molecular weight polybenzimidazole membranes for high temperature PEMFC. *Fuel Cells*, 14(1): 7-15.
22. Cobridge, D. E. C. (1995). Phosphorus: an outline of chemistry, biochemistry and uses. *Studies in Inorganic Chemistry*: pp. 20.
23. Gopalsamy, B. M., Mondal, B., and Ghosh, S. (2009). Taguchi method and ANOVA: An approach for process parameters optimization ofhard machining while machining hardened steel. *Journal of Scientific and Industrial Research,* 68(8): 686-695.

24. Sousa, S. I. V., Martins, F. G., Alvim-Ferraz, M. C. M. and Pereira, M. C. (2007). Multiple linear regression and artificial neural networks based on principal components to predict ozone concentrations. *Environmental Modelling & Software*, 22(1): 97-103.
25. Andrews, D. F. (1974). A robust method for multiple linear regression. *Technometrics*, 16(4): 523-531.
26. Suherman, H. (2017). Optimization of internal mixing parameter on the electrical conductivity of multiwall carbon nanotubes/synthetic graphite/epoxy nanocomposites for conductive polymer composites using Taguchi method. *Jurnal Kejuruteraan*, 29(2): 79-85.
27. Mahapatra, S. S. and Patnaik, A. (2006). Parametric optimization of wire electrical discharge machining (WEDM) process using Taguchi method. *Journal of the Brazilian Society of Mechanical Sciences and Engineering*, 28(4): 422-429.
28. Kamaruddin, S., Khan, Z. A. and Foong, S. H. (2010). Application of Taguchi method in the optimization of injection moulding parameters for manufacturing products from plastic blend. *International Journal of Engineering and Technology*, 2(6): 574-530.